



Methods and Model Dependency of Extreme Event Attribution: The 2015 European Drought

Journal Article

Author(s):

[Hauser, Mathias](#) ; Gudmundsson, Lukas; Orth, René; Jézéquel, Didier; Haustein, Karsten; Vautard, Robert; Van Oldenborgh, Geert J.; Wilcox, Laura J.; [Seneviratne, Sonia I.](#) 

Publication date:

2017-10

Permanent link:

<https://doi.org/10.3929/ethz-b-000212504>

Rights / license:

[Creative Commons Attribution-NonCommercial-NoDerivatives 4.0 International](#)

Originally published in:

Earth's Future 5(10), <https://doi.org/10.1002/2017EF000612>



RESEARCH ARTICLE

10.1002/2017EF000612

Methods and Model Dependency of Extreme Event Attribution: The 2015 European Drought

Mathias Hauser¹, Lukas Gudmundsson¹, René Orth¹, Aglaé Jézéquel², Karsten Haustein³, Robert Vautard², Geert J. van Oldenborgh⁴, Laura Wilcox⁵, and Sonia I. Seneviratne¹

Key Points:

- Multi-method event attribution of the 2015 European drought
- Contradicting evidence on the role of anthropogenic influence on the event
- Uncertainty in event attribution may be larger than previously thought

Supporting Information:

- Supporting Information S1

Corresponding author:

M. Hauser, mathias.hauser@env.ethz.ch

Citation:

Hauser, M., Gudmundsson, L., Orth, R., Jézéquel, A., Haustein, K., Vautard, R., van Oldenborgh, G. J., Wilcox, L., & Seneviratne, S. I. (2017). Methods and model dependency of extreme event attribution: The 2015 European drought. *Earth's Future*, 5, 1034–1043, <https://doi.org/10.1002/2017EF000612>

Received 15 MAY 2017

Accepted 13 SEP 2017

Accepted article online 20 SEP 2017

Published online 20 OCT 2017

© 2017 The Authors.

This is an open access article under the terms of the Creative Commons Attribution-NonCommercial-NoDerivs License, which permits use and distribution in any medium, provided the original work is properly cited, the use is non-commercial and no modifications or adaptations are made.

¹Institute for Atmospheric and Climate Science, ETH Zurich, Zurich, Switzerland, ²LSCE, l'Orme des Merisiers, UMR 8212 CEA-CNRS-UVSQ, U Paris-Saclay, IPSL, Gif-sur-Yvette, France, ³Environmental Change Institute, University of Oxford, Oxford, UK, ⁴Royal Netherlands Meteorological Institute (KNMI), De Bilt, Netherlands, ⁵National Centre for Atmospheric Science (Climate), Department of Meteorology, University of Reading, Reading, UK

Abstract Science on the role of anthropogenic influence on extreme weather events, such as heat-waves or droughts, has evolved rapidly in the past years. The approach of “event attribution” compares the occurrence-probability of an event in the present, factual climate with its probability in a hypothetical, counterfactual climate without human-induced climate change. Several methods can be used for event attribution, based on climate model simulations and observations, and usually researchers only assess a subset of methods and data sources. Here, we explore the role of methodological choices for the attribution of the 2015 meteorological summer drought in Europe. We present contradicting conclusions on the relevance of human influence as a function of the chosen data source and event attribution methodology. Assessments using the maximum number of models and counterfactual climates with pre-industrial greenhouse gas concentrations point to an enhanced drought risk in Europe. However, other evaluations show contradictory evidence. These results highlight the need for a multi-model and multi-method framework in event attribution research, especially for events with a low signal-to-noise ratio and high model dependency such as regional droughts.

1. Introduction

Event attribution is a quickly growing field (Herring et al., 2016; Stott et al., 2016; National Academies of Sciences, Engineering, and Medicine (NAS), 2016) with high visibility and potential key implications. It has, for instance, been suggested that evidence from event attribution research could be used in courts of law to obtain reparations following impacts of extreme weather events (Allen, 2003; Thompson & Otto, 2015; Stott et al., 2016). In event attribution, a change in the occurrence probability of an extreme event is quantified with the Risk Ratio (NAS, 2016), $RR = p_f/p_c$, where p_f is the probability of the event in the factual climate including climate change, and p_c the probability of the same event in a counterfactual climate without anthropogenic climate change (Figure 1). This probabilistic framing is suited for events defined via the exceedance of a threshold of a weather variable, which always have some stochastic behavior. The observed event is thereby only used to define the threshold, and different meteorological situations could lead to events of the same magnitude. Although event attribution assessments are sensitive to methodological choices (Lewis & Karoly, 2013; Shiogama et al., 2013; Otto et al., 2015; Uhe et al., 2016), it is still common to rely on a limited number of models and methods (Sippel et al., 2016; Dong et al., 2016; Schaller et al., 2016; Mitchell et al., 2016). In this study, we analyze the role of methodological choices for the attribution of the 2015 European drought.

In the summer of 2015, Central Europe experienced a pronounced drought and heat wave. The event broke local temperature records (Dong et al., 2016; Sippel et al., 2016), and was characterized by very low precipitation (Orth et al., 2016), which resulted in significantly reduced surface water availability (Van Lanen et al., 2016; Laaha et al., 2016). While the extreme temperatures occurring during that event were shown to have a larger probability due to climate change (Dong et al., 2016; Sippel et al., 2016), the role of human influence on the meteorological drought (precipitation deficit) has not yet been assessed.

The use of general circulation models (GCMs) is central in event attribution studies. They allow the computation of large ensembles of the factual climate as well as of the counterfactual climate, for which

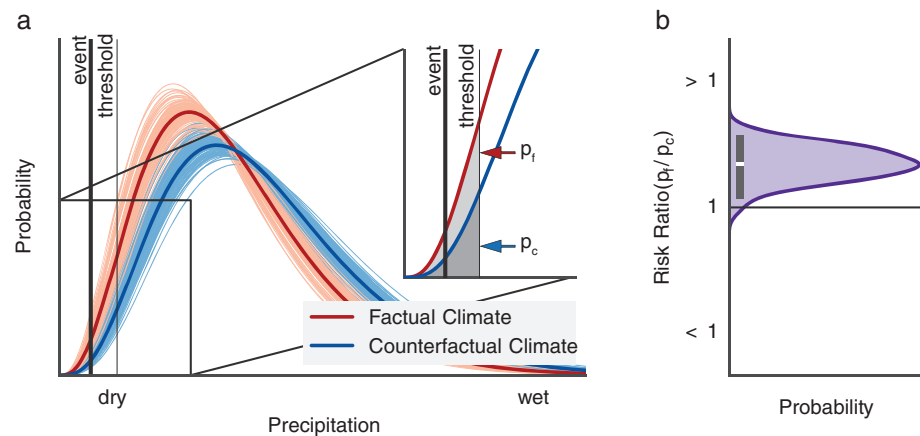


Figure 1. Probabilistic event attribution and the risk ratio. (a) Hypothetical Probability Density Functions (PDFs) of precipitation in the factual (red) and counterfactual (blue) climate. The thin, light lines indicate parameter uncertainty of the two PDFs. The magnitude of the investigated extreme event is indicated with the thick black line. To avoid a selection bias, we use the second largest event on the observational record as threshold, shown with the thin black line. (Inset) The parameters p_f and p_c are calculated as the gray area under the PDF. (b) PDF of the RR, taking the parameter uncertainty into account (magenta), 95% credibility interval (black bar), and best estimate (median, white line).

no observations exist. However, using GCMs also involves a number of methodological choices, potentially influencing the RRs obtained from them. In this study, we will assess the influence of the following choices on the RR: different counterfactual climates (as defined by different levels of anthropogenic forcing agents: greenhouse gases (GHGs) and aerosols), the selection of the climate model, the representation of sea surface temperatures (SSTs), and additionally the effect of using different datasets for observation-based RRs.

2. Factual and Counterfactual Climate

The factual climate (referred to as PRES, hereafter) should represent the “real”, current, climate conditions as accurately as possible. Here, it is estimated from simulations forced with boundary conditions (GHGs, aerosols, and potentially SSTs) representing observed, current-day values. The counterfactual climate, on the other hand, should represent a climate undisturbed by human influence. Four possibilities have been introduced in the scientific literature, which we will refer to as PAST, PAST_GHG, NAT, and piC, hereafter (Table 1). PAST consists of historical simulations forced with observed boundary conditions, but uses a time period from the middle of the 20th century, when the human imprint on climate was smaller. In this study, we use the 1960s as historical period, when the anthropogenic GHG forcing was about one-third of the current forcing. In contrast to anthropogenic GHG forcing, the anthropogenic aerosols load was not (quasi)monotonically increasing. In the 1960s, the European tropospheric sulfate load was much higher than in pre-industrial times, and also than nowadays (Figure S1, Supporting Information). Aerosols were found to influence precipitation globally and for certain regions (Wilcox et al., 2013; Polson et al., 2014). Therefore, RRs are subject to changes caused by direct and indirect aerosol effects which may not be appropriately attributed when using PAST only. Thus, we consider a second set of simulations including anthropogenic GHG emissions, but using constant, pre-industrial aerosol concentrations (GHG-only simulations). As these simulations still include anthropogenic GHG emissions, we also need to consider a historical period as counterfactual climate (PAST_GHG). Analyzing the difference between PAST and PAST_GHG allows us to compare the effect of aerosols on European precipitation. The next counterfactual climate, NAT, is forced by observed solar and volcanic boundary conditions, but GHG and aerosol concentrations are set to pre-industrial levels (i.e., historical natural simulations). The third counterfactual climate, piC, is obtained from pre-industrial control simulations. These are freely evolving simulations with GHG concentrations and anthropogenic aerosol emissions representative for the year 1850 but without historical natural forcing variations, notably volcanic eruptions.

Besides the choice of the counterfactual climate, the selection of the GCM (or GCMs) is also expected to influence the outcome of an attribution study. Furthermore, the degree of conditioning of the GCM will

Table 1. Overview of Observation- and Model-Based Event Attribution Methods. SST_{OBS} Is an Observed SST (Sea Surface Temperature) Dataset and ΔSST is the Change in SSTs Due to Climate Change, Derived from Models in the Coupled Model Intercomparison Project (CMIP5)

Data basis	Name	Factual climate (p_f) (with climate change)	Counterfactual climate (p_c) (without climate change)
Models	PRES vs. PAST	Anthropogenic forcing simulation of present-day period with: (1) Interactive SSTs (2) Prescribed SST_{OBS}	Anthropogenic forcing simulation of past time period (1960s) with: (1) Interactive SSTs (2) Prescribed SST_{OBS}
	PRES vs. PAST_GHG	Anthropogenic forcing simulation of present-day period with: (1) Interactive SSTs (2) Prescribed SST_{OBS}	GHG-only forcing simulation of past time period (1960s) with: (1) Interactive SSTs (2) Prescribed SST_{OBS} ^a
	PRES vs. NAT	Anthropogenic forcing simulation of present-day period with: (1) Interactive SSTs (2) Prescribed SST_{OBS}	Natural forcing simulations of present-day period with: (1) Interactive SSTs (2) Prescribed $SST_{OBS} - \Delta SST$
	PRES vs. piC	Anthropogenic forcing simulation of present-day period with: (1) Interactive SSTs	Natural forcing simulation of pre-industrial time period with: (1) Interactive SSTs
Observations	Regression-based	Present	Past (e.g., 1960s)

^aNo simulations of this kind are used in this study.

influence the estimate of the RRs. Specifically, SSTs can either be interactively computed by the model or prescribed, for instance from observations. Thus, we will also contrast RRs from models with interactive and prescribed SSTs. An additional possibility is provided by simulations where regional climate models (RCMs) are used to dynamically downscale the generally coarse-resolution GCM output.

3. Methods and Data

3.1. Computation of Risk Ratios

As a result of diverse availability of sample sizes, we use different methods to calculate RRs from models and observations. For the model-based RR, we assume that the precipitation data follows a gamma distribution (Stagge et al., 2015). We fit one gamma distribution to the simulated factual precipitation, and another to the counterfactual precipitation. From these two gamma distributions, we compute the probability that the precipitation amount will be below the chosen threshold, in the factual climate (p_f) and the counterfactual climate (p_c). We calculate uncertainties in a Bayesian setting and use a Markov Chain Monte Carlo (MCMC) sampler that is affine-transformation invariant (Goodman & Weare, 2010; Foreman-Mackey et al., 2013) to estimate the parameters of the gamma distributions. Starting from non-informative priors, the converged posterior distributions (50,000 non-independent samples) give an estimate of the parameter uncertainty.

For the observation-based event attribution, we follow a recent study (Gudmundsson & Seneviratne, 2016) and fit the precipitation data to a generalized linear model (GLM; McCullagh & Nelder, 1989) with global mean temperature as covariate, assuming a logarithmic link function and gamma distributed residuals. Global mean temperature from a global surface temperature dataset is smoothed with a LOWESS (locally weighted scatterplot smoothing) filter (Cleveland, 1979; using 5% of the data) to minimize the influence of the El Niño-Southern Oscillation (van Oldenborgh, 2007). For the factual climate (p_f), we insert the global mean temperature of 2015 into the GLM. For the counterfactual climate (p_c), we use the average

temperature between 1960 and 1969. The same MCMC algorithm as for the model-based RR is used to calculate the posterior distribution. The return time of the event is calculated as the inverse of the probability of staying below precipitation of the event (p_f^{-1}).

3.2. Observation Data

To assess the uncertainty in observed precipitation, we consider four observational datasets: (1) the European Climate Assessment and Dataset (ECAD) E-OBS dataset (Haylock et al., 2008), (2) the National Oceanic and Atmospheric Administration's (NOAA) PREcipitation REConstruction over Land (PREC/L, Chen et al., 2002), (3) the Climate Prediction Center (CPC) Merged Analysis of Precipitation (CMAP; Xie & Arkin, 1997), and (4) the Climatic Research Unit (CRU) Time Series dataset (CRU TS, Harris et al., 2014). We employ the Goddard Institute for Space Studies (GISS) analysis of global surface temperature (GISTEMP, Hansen et al., 2010) as our global mean temperature dataset.

3.3. Model Data

For the model-based assessment of European drought risk, we use simulations from a total of 23 climate models. Three types of models are considered: GCMs which have interactive SSTs, GCMs with prescribed SSTs, and RCMs downscaling the output of GCMs.

Most of the considered models (19) have interactive SSTs and stem from the Coupled Model Intercomparison Project, Phase 5 (CMIP5; Taylor et al., 2012, Table S1). The factual climate (PRES) is estimated with simulations forced with the representative concentration pathway (RCP) 8.5 scenario (Meinshausen et al., 2011), because the historical simulations from CMIP5 end in 2005. RCP8.5 deviates slightly from the observations by now, however, the differences between the scenarios are not relevant until after 2030 (Kirtman et al., 2013). The modeled SSTs in the CMIP5 simulations do not correspond to the observed SSTs in the corresponding year, therefore we use a 20-year window around the event (2006–2025 for PRES). For PAST, we use historical simulations and select the years from 1951 to 1970. PAST_GHG is obtained from GHG-only simulations (also using 1951–1970), to assess the importance of aerosols for European precipitation within CMIP5. NAT is estimated from historical natural CMIP5 simulations. As these end in 2005, we select the years from 1986 to 2005. Finally, for piC, we use the last 200 years of the longest pre-industrial control simulation from each model, such that all GCMs contribute the same number of data points and the end point is closest to the starting point of the historical simulations to minimize the effects of model drift.

Two atmosphere-only models, namely HadGEM3-A and HadAM3P (as employed in the weather@home, w@h, volunteer-distributed modeling framework) (Massey et al., 2015) are used in our analysis (Text S1 and S2). Both models prescribe SSTs. They are forced with observed SSTs and sea ice at the lower boundary in order to simulate the factual climate. For the counterfactual climate, a climate change signal (Δ SST) is removed from the SST observations. Δ SST is derived from historical and historical-natural CMIP5 simulations. For HadGEM3-A, Δ SST is estimated from the multi-model mean, while for w@h 11 individual CMIP5 models are used (Schaller et al., 2016). Natural sea ice conditions are estimated by either using the maximum observed sea ice extent (for w@h, the winter of 1986/1987 as the employed dataset starts in 1985) or via the observed relationship between observed temperature and ice-coverage (HadGEM3-A). The last two of the 23 considered models are RCMs from the Coordinated Downscaling Experiment over the European Domain (EURO-CORDEX, Jacob et al., 2014). Each RCM is forced with boundary conditions from historical and RCP8.5 simulations from five GCMs participating in CMIP5 (Text S3).

3.4. Post-processing

All observational and model data undergoes the same post-processing. We first calculate cumulative June-to-August (JJA) precipitation on land, area-averaged over the Central European region defined in the Special Report on Managing the Risks of Extreme Events and Disasters to Advance Climate Change Adaptation (SREX, Seneviratne et al., 2012) on the original grid of each dataset. All area-averaged data (models and observations) are then bias-corrected using a power transformation (Gudmundsson et al., 2012) to best match the cumulative density function of the E-OBS dataset for the period 1965–2013 (1985–2013 for the w@h simulations and 1971–2013 for the RCM simulations). This is done for every model individually, pooling all available ensemble members. The same bias correction is then applied to the counterfactual simulations.

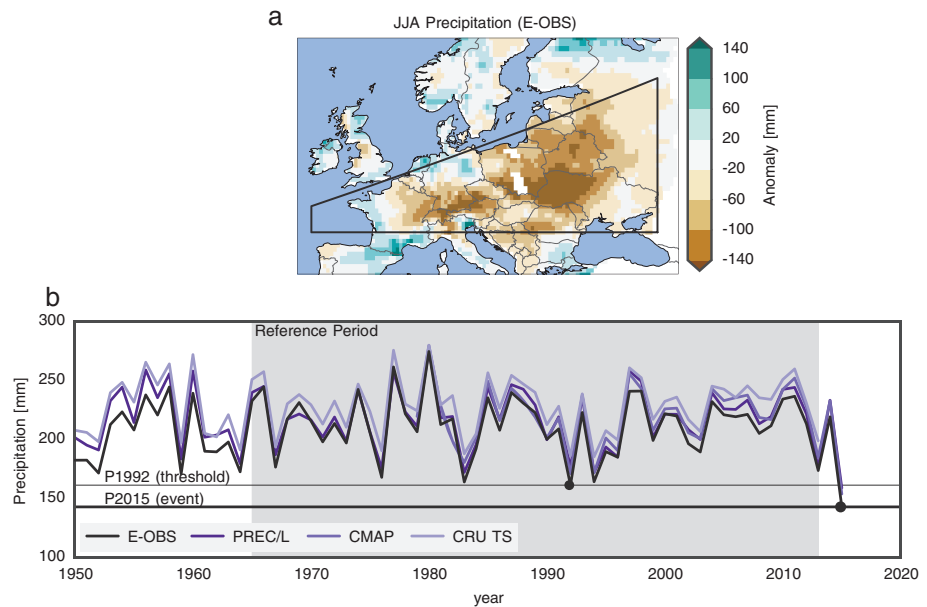


Figure 2. Precipitation in Central Europe. (a) Map of precipitation anomaly over Europe for the summer of 2015 (June-to-August (JJA), relative to 1965–2013). The black outline shows the study region. (b) Absolute precipitation over the study region for four observational datasets (see Section 3.2). The horizontal lines denote the lowest (P2015, thick line) and second lowest (P1992, thin line) observed precipitation in the E-OBS dataset. We use P1992 as threshold to compute p_f and p_c (see Figure 1). The gray shading indicates the reference period (1965–2013).

4. Results

The cumulative precipitation anomaly in Central Europe was very large in 2015, it was smaller than -140 mm in some regions (Figure 2a). Averaged over the target area, 2015 was the driest year on the observational record (Figure 2b and Orth et al., 2016). To assess the anthropogenic influence on this event, we estimate the probability of staying below a precipitation threshold in the factual (p_f) and counterfactual (p_c) climate. As threshold, we choose the largest observed event *before* 2015 (Figure 2b) to avoid a selection bias (Stott et al., 2004). Thus, we do not estimate the RR for the exact event, but for a class of events more severe than the driest summer before 2015.

We start our assessment with GCM simulations with interactive SSTs (i.e., a fully coupled ocean) obtained from CMIP5. Although the multi-model mean precipitation over Europe shows only a small bias (Flato et al., 2013), individual models exhibit considerable offsets (Figure S2), which we correct for (Section 3.4). The assumption of gamma-distributed data is visually assessed with quantile–quantile (QQ) plots of the historical simulations (Figure S3). The QQ plots give high confidence that the gamma distribution is appropriate to describe the used rainfall data. To derive a comprehensive attribution statement with several GCMs, it is common to pool individual models (Lewis & Karoly, 2013). In Figure 3a, we present two model pools based on all used CMIP5 members: (1) every ensemble member of each model (Table S1), and (2) one ensemble member of each model (to assign each model equal weight). Comparing the factual climate to the pre-industrial control simulations (PRES vs. piC) indicates a strong human contribution to the 2015 drought when considering all ensemble members, but not when considering one ensemble member per model. In contrast, an anthropogenic influence on European drought risk is uniformly suggested when using historical natural simulations as counterfactual climate (PRES vs. NAT). Note that, PRES and NAT do not share the same base period, and consequently their natural forcing differs, especially the volcanic aerosols. However, aligning the base period by using the years from 1986 to 2005 for PRES, changes the RRs only slightly (Figure S4a). Finally, with a historical period as counterfactual climate (PRES vs. PAST and PRES vs. PAST_GHG), the pooled CMIP5 ensembles indicate no human influence on precipitation. Additionally, we show a RR derived from 10 high-resolution RCM simulations, but only PRES versus PAST can be compared, as no simulations without anthropogenic forcing are available. The RCM-based assessment conforms to the CMIP5-derived RRs (PRES vs. PAST) and yields no detectable precipitation signal. Note that, however, PAST includes the high

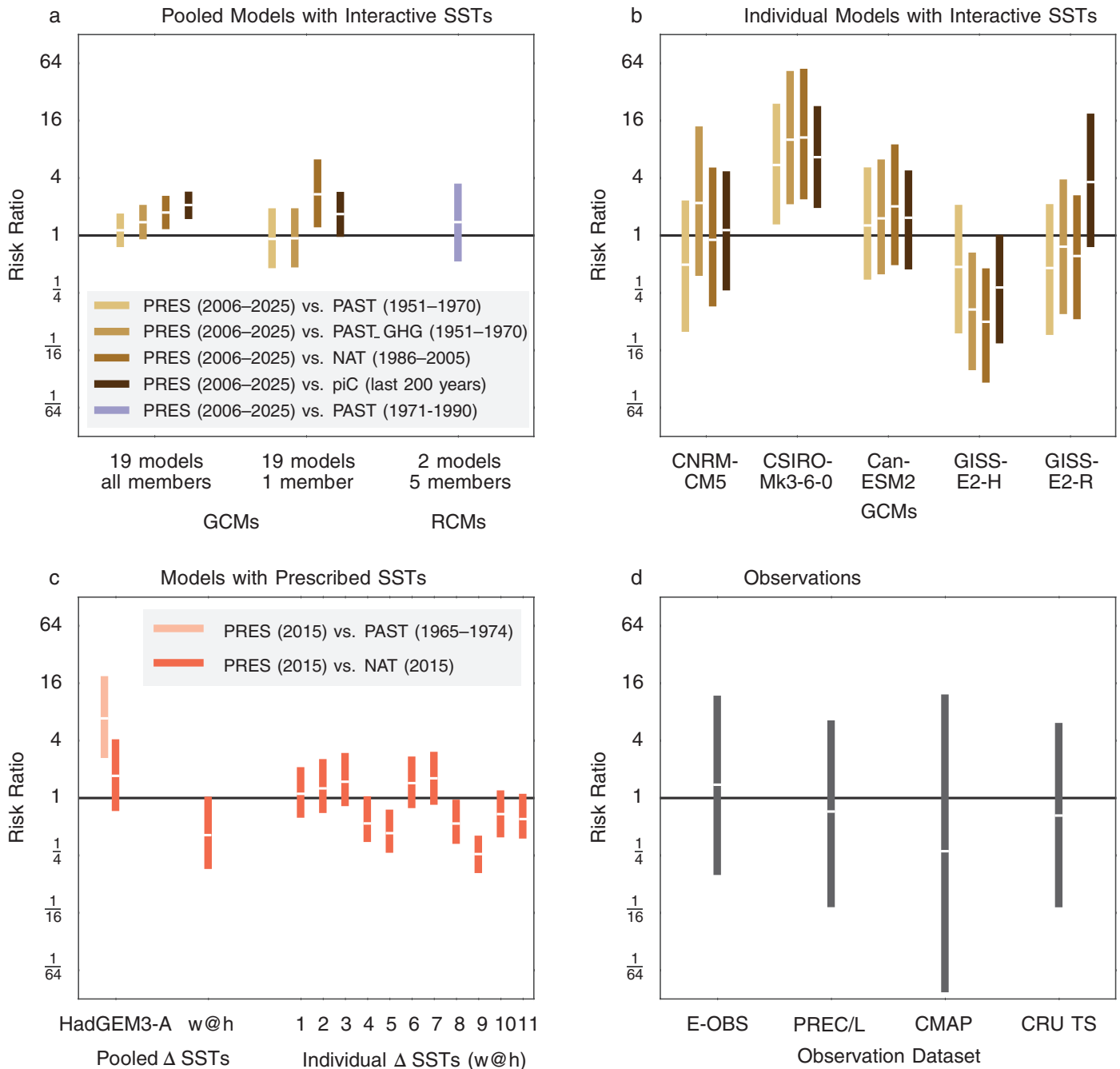


Figure 3. Risk ratios (RRs) for all model simulations, datasets, and counterfactual climates considered in this study. Bars show the best estimate (median) and 95% credibility interval of RR on a logarithmic axis. Dates in the legends indicate years used to estimate p_f and p_c , respectively. (a) Pooled general circulation models (GCMs) with interactive sea surface temperatures (SSTs) from the Coupled Model Intercomparison Project, Phase 5 (CMIP5), and regional climate models from the Coordinated Downscaling Experiment over the European Domain (EURO-CORDEX) for four counterfactual climates (Table 1). (b) Individual GCMs (from CMIP5) with five ensemble members each. (c) Model simulations with prescribed SSTs. On the left HadGEM3-A and the pooled w@h simulations. On the right all 11 w@h simulations forced with individual Δ SST patterns. (d) RRs for four observational datasets. See Table S2 to Table S4.

aerosol levels present during this time period (Figure S1). These comparisons show a first striking result. Namely, that the choice of the counterfactual climate used as a baseline can strongly affect the conclusions reached with respect to event attribution.

While the choice of counterfactual climate was found to be central to the result, we also expect that the results are dependent on the considered models. We assess the inter-model spread for the five GCMs with at least five ensemble members (Figure 3b). For PRES versus piC, only one out of the five models show significantly increased RRs. Using NAT as counterfactual climate yields RRs with a particularly large range. Three models suggest no change in drought risk, one (CSIRO-Mk3-6-0) indicates a doubling of the drought risk (lower uncertainty bound), while another (GISS-E2-H) suggests half the drought risk (upper uncertainty bound). PRES versus PAST_GHG yields similar RRs to PRES versus NAT. Finally, for PRES versus PAST the model results mostly conform to the multi-model RRs. Only CSIRO-Mk3-6-0 suggests an attributable increase in drought probability. Aligning the base period for PRES to the base period of NAT increases the RRs for all models, except CAN-ESM2 (Figure S4b). In essence, different subsets of CMIP5 models and counterfactual climates produce different attribution statements.

Next, we assess GCM simulations with prescribed SSTs (HadGEM3-A and w@h), where ocean temperatures are used as lower boundary condition. European summer precipitation is close to observations in Europe for HadGEM3-A (Figure S2), but w@h shows a large absolute bias and overestimates variability (Massey et al., 2015). Therefore, we also bias-corrected these simulations. Comparing PRES versus NAT for HadGEM3-A and the pooled w@h simulations yields a RR that is indistinguishable from one—no human influence is detectable (Figure 3c). The w@h simulations highlight the important role of different Δ SST patterns. Eight of them yield no significant change in drought risk, but the other three indicate a reduced drought probability. A comparison of w@h simulations under GHG-only, PRES, and NAT conditions (Figure S5) indicates that the anthropogenic increase in GHGs led to a drying, while the higher aerosol load caused a wettening. These changes are likely linked to the projected expansion of the extratropical zone of higher pressure which is particularly sensitive to rainfall changes over the Mediterranean region in summer in the current generation of GCMs, including HadGEM3-A and w@h. Thus, it may well be that the mostly-insignificant RRs are due to the compensating effect of GHGs and aerosols in these models. The w@h simulations only start in 1985, therefore we cannot compare PRES versus PAST. In HadGEM3-A, PRES versus PAST points to an increased drought risk and is highly significant. This could either be due to the different aerosol concentrations between the periods or because of negative precipitation trends in HadGEM3-A, which are in disagreement with observations (not shown).

Finally, we perform an observation-based event attribution analysis with four datasets (Figure 3d). Precipitation is regressed against smoothed global mean temperature, which is considered a proxy of climate change (van Oldenborgh, 2007; Otto et al., 2012; Gudmundsson & Seneviratne, 2016). The observation-based RRs have comparatively large confidence intervals, the RRs range from 0.01 to 13.4 (95% confidence interval), and none of the datasets indicate a change in Central European drought risk, in line with Gudmundsson and Seneviratne (2016). Using only global mean temperature in the regression analysis ignores potential aerosol effects, although they can influence regional-global precipitation (see discussion in Section 2). In fact, comparing the precipitation and the anthropogenic aerosol time series (Figure S1a and S1c), gives no indication of such a relationship operating in Europe, and a regression analysis confirms this. Years following large volcanic eruptions often have small precipitation amounts (Figure S1a and S1b), in line with earlier findings (e.g. Iles & Hegerl, 2015). This is not directly relevant for 2015, as no major volcanic eruption happened in the past few years. However, to rule out that the influence of the volcanoes could mask a trend in the regression, we re-computed the regression analysis, excluding years with high stratospheric aerosol concentrations, and still found no significant signal of global mean temperature or anthropogenic aerosols. Precipitation trends are not homogeneous in Central Europe—they tend to be positive in the east and negative in the west (not shown). However, even when splitting the region into a western and eastern part, no human influence is detected in the observations. The return time of the precipitation amount in 2015 is larger than 90 years (lower uncertainty bound at the 2.5th percentile). Results with an alternative observation-based methodology also show only a small precipitation difference between a recent and past time period, and are thus consistent with the regression-based assessment (Figure S6). This second method evaluates the thermodynamic effect of climate change (Analogue Method, Text S4).

5. Conclusions

The comprehensive assessment to attribute a human impact on the 2015 European summer drought presented in this study illustrates the complexity of the exercise. We find that the drought could be *more likely*, *less likely*, or *unaffected* by anthropogenic forcing, depending on the methodology and data source. Thus, we are not able to conclusively determine whether the 2015 drought was attributable to anthropogenic forcing. We note, however, that the RR with the largest signal-to-noise ratio, obtained by maximizing the number of considered models (whole CMIP5 ensemble) and using the largest forcing difference (through using pre-industrial GHG concentrations), suggests a detectable human influence on the likelihood of Central European droughts. This result should not be overstated though: the uncertainty of the multi-model assessment could be too small, as the individual models are not fully independent (Knutti et al., 2013). Additionally, great care has to be taken when interpreting results from pre-industrial control simulations, as natural forcings can be different from historical simulations (Taylor et al., 2012) and some models may have drift. We try to minimize the effect of model drift by using the last years of the pre-industrial control simulations. Note that RRs are indeed sensitive to the time period used from the pre-industrial control simulations (Figure S7). Using the mid-20th century as counterfactual climate (PRES vs. PAST and the observations), on the other hand, may underestimate the climate change signal, because one-third of the GHG forcing, and a large part of the anthropogenic aerosol forcing occurred before this period. When tested with CMIP5, however, the net effect was found to be negligible (Figure S8). The effect of aerosols on Central European precipitation was found to be small. Nonetheless, anthropogenic and volcanic aerosols can influence the climate (Chalmers et al., 2012; Wilcox et al., 2013; Iles & Hegerl, 2015), and its influence may need to be considered in extreme event attribution. Furthermore, our analysis reveals a strong model dependency, consistent with earlier findings for drought projections (Orlowsky & Seneviratne, 2013). Additionally, GCMs miss some observed precipitation trends, especially near coasts (van Haren et al., 2013). Finally, precipitation has a large interannual variability, which may mask existing trends (Orlowsky & Seneviratne, 2013). We restricted our analysis to meteorological droughts and would expect a stronger anthropogenic signal in other hydrological variables with a tighter link to temperature (e.g. soil moisture or precipitation minus evapotranspiration).

In this study, we highlight that any event attribution statement can—and will—critically depend on the researcher's decision regarding the framing of the attribution analysis, in particular with respect to the choice of model, counterfactual climate, and boundary conditions. This suggests that single-model assessments could overlook, or falsely detect signals, even when using a large number of ensemble members, an approach commonly applied in the literature (Otto et al., 2012; Sippel et al., 2016; Dong et al., 2016; Schaller et al., 2016; Mitchell et al., 2016). Our results also emphasize the difficulty of attributing drought events, even for an event as extreme as the 2015 drought, an aspect possibly underestimated in the research community (NAS, 2016) but in line with findings from other drought attribution studies (Shiogama et al., 2013; King et al., 2014; Kelley et al., 2015; Wilcox et al., 2015; Otto et al., 2015; Gudmundsson & Seneviratne, 2016). In the view of the consideration of event attribution in legal frameworks, it is thus crucial to assess human influence on climate extremes using multi-model and multi-method based event attribution.

References

- Allen, M. (2003). Liability for climate change. *Nature*, 421(6926), 891–892. <https://doi.org/10.1038/421891c>.
- Chalmers, N., Highwood, E. J., Hawkins, E., Sutton, R., & Wilcox, L. J. (2012). Aerosol contribution to the rapid warming of near-term climate under RCP 2.6. *Geophysical Research Letters*, 39. <https://doi.org/10.1029/2012GL052848>
- Chen, M., Xie, P., Janowiak, J., & Arkin, P. (2002). Global land precipitation: A 50-yr monthly analysis based on gauge observations. *Journal of Hydrometeorology*, 3(3), 249–266. [https://doi.org/10.1175/1525-7541\(2002\)003<249:GLPAYM>2.0.CO;2](https://doi.org/10.1175/1525-7541(2002)003<249:GLPAYM>2.0.CO;2).
- Cleveland, W. (1979). Robust locally weighted regression and smoothing scatterplots. *Journal Of The American Statistical Association*, 74(368), 829–836. <https://doi.org/10.2307/2286407>
- Dong, B., Sutton, R., Shaffrey, L., & Wilcox, L. (2016). The 2015 European heat waves. *Bulletin of the American Meteorological Society*, 97, S57–S62. <https://doi.org/10.1175/BAMS-D-16-0140.1>
- Flato, G., Marotzke, J., Abiodun, B., Braconnot, P., Chou, S., Collins, W., ... Rummukainen, M. (2013). *Evaluation of Climate Models*, book section 9 (pp. 741866). Cambridge, United Kingdom and New York, NY: Cambridge University Press. <https://doi.org/10.1017/CBO9781107415324.020>
- Foreman-Mackey, D., Hogg, D. W., Lang, D., & Goodman, J. (2013). emcee: The MCMC hammer. *Publications of the Astronomical Society of the Pacific*, 125, 306–312. <https://doi.org/10.1086/670067>
- Goodman, J., & Weare, J. (2010). Ensemble samplers with affine invariance. *Communications in Applied Mathematics and Computational Science*, 5(1), 65–80. <https://doi.org/10.2140/camcos.2010.5.65>

Acknowledgments

We acknowledge the E-OBS dataset from the EU-FP6 project ENSEMBLES (<http://ensembles-eu.metoffice.com>) and the data providers in the ECA&D project (<http://www.ecad.eu>). We acknowledge the World Climate Research Programme's Working Group on Coupled Modeling, which is responsible for CMIP, and we thank the climate modeling groups (listed in Table S1) for producing and making available their model output. For CMIP the U.S. Department of Energy's Program for Climate Model Diagnosis and Intercomparison provides coordinating support and led development of software infrastructure in partnership with the Global Organization for Earth System Science Portals. We also thank the volunteers who donated their computing time to weather at home. This work is supported by EU-FP7 grant No. 607085-EUCLEIA. We also acknowledge partial support from the ERC DROUGHT-HEAT project (Contract No. 617518). A.J. is supported by EU-FP7 grant No. 338965-A2C2. E-OBS is accessible from <http://www.ecad.eu>. PREC/L was obtained from <https://www.esrl.noaa.gov/psd/data/gridded/data.prcr.html>. CMAP was retrieved from <https://www.esrl.noaa.gov/psd/data/gridded/data.cmap.html>. The CRU TS data is stored at: <http://browse.ceda.ac.uk/browse/badc/cru>. GISTEMP can be downloaded from <http://data.giss.nasa.gov/gistemp/>. We acknowledge Jan Sedláček's post-processing of CMIP5 data (<https://data.iac.ethz.ch/atmos/>). HadGEM is distributed via the C20C+ archive (<http://portal.nersc.gov/c20c/>). The weather at home data is available upon request.

- Gudmundsson, L., Bremnes, J. B., Haugen, J. E., & Engen-Skaugen, T. (2012). Technical note: Downscaling RCM precipitation to the station scale using statistical transformations - a comparison of methods. *Hydrology and Earth System Sciences*, *16*(9), 3383–3390. <https://doi.org/10.5194/hess-16-3383-2012>
- Gudmundsson, L., & Seneviratne, S. I. (2016). Anthropogenic climate change affects meteorological drought risk in Europe. *Environmental Research Letters*, *11*(4). <https://doi.org/10.1088/1748-9326/11/4/044005>
- Hansen, J., Ruedy, R., Sato, M., & Lo, K. (2010). Global surface temperature change. *Reviews of Geophysics*, *48*. <https://doi.org/10.1029/2010RG000345>
- Harris, I., Jones, P. D., Osborn, T. J., & Lister, D. H. (2014). Updated high-resolution grids of monthly climatic observations - the CRU TS3.10 dataset. *International Journal of Climatology*, *34*(3), 623–642. <https://doi.org/10.1002/joc.3711>
- Haylock, M. R., Hofstra, N., Tank, A. M. G. K., Klok, E. J., Jones, P. D., & New, M. (2008). A European daily high-resolution gridded data set of surface temperature and precipitation for 1950–2006. *Journal of Geophysical Research-Atmospheres*, *113*(D20). <https://doi.org/10.1029/2008JD010201>
- Herring, S. C., Hoell, A., Hoerling, M. P., Kossin, J. P., III, C. J. S., & Stott, P. A. (Eds.) (2016). Explaining extreme events of 2015 from a climate perspective. *Bulletin of the American Meteorological Society*, *97*, S1–S145. <https://doi.org/10.1175/BAMS-ExplainingExtremeEvents2015.1>
- Iles, C. E., & Hegerl, G. C. (2015). Systematic change in global patterns of streamflow following volcanic eruptions. *Nature Geoscience*, *8*(11), 838–842. <https://doi.org/10.1038/NGEO2545>
- Jacob, D., Petersen, J., Eggert, B., Alias, A., Christensen, O. B., Bouwer, L. M., ... Yiou, P. (2014). EURO-CORDEX: New high-resolution climate change projections for European impact research. *Regional Environmental Change*, *14*(2, SI), 563–578. <https://doi.org/10.1007/s10113-013-0499-2>
- Kelley, C. P., Mohtadi, S., Cane, M. A., Seager, R., & Kushnir, Y. (2015). Climate change in the fertile crescent and implications of the recent Syrian drought. *Proceedings of the National Academy of Sciences of the United States of America*, *112*(11), 3241–3246. <https://doi.org/10.1073/pnas.1421533112>
- King, A. D., Karoly, D. J., Donat, M. G., & Alexander, L. V. (2014). Climate change turns Australia's 2013 big dry into a year of record-breaking heat. *Bulletin of the American Meteorological Society*, *95*(9, S), S41–S45.
- Kirtman, B., Power, S., Adedoyin, J., Boer, G., Bojariu, R., Camilloni, I., ... Wang, H. (2013). *Near-Term Climate Change: Projections and Predictability*, book section 11 (pp. 9531028). Cambridge, United Kingdom and New York, NY: Cambridge University Press. <https://doi.org/10.1017/CBO9781107415324.023>
- Knutti, R., Masson, D., & Gettelman, A. (2013). Climate model genealogy: Generation CMIP5 and how we got there. *Geophysical Research Letters*, *40*(6), 1194–1199. <https://doi.org/10.1002/grl.50256>
- Laaha, G., Gauster, T., Tallaksen, L. M., Vidal, J.-P., Stahl, K., Prudhomme, C., ... Wong, W. K. (2016, 2016). The european 2015 drought from a hydrological perspective. *Hydrology and Earth System Sciences Discussions*, 1–30. <https://doi.org/10.5194/hess-2016-366>
- Lewis, S. C., & Karoly, D. J. (2013). Anthropogenic contributions to Australia's record summer temperatures of 2013. *Geophysical Research Letters*, *40*(14), 3705–3709. <https://doi.org/10.1002/grl.50673>
- Massey, N., Jones, R., Otto, F. E. L., Aina, T., Wilson, S., Murphy, J. M., Hassell, D., Yamazaki, Y. H., & Allen, M. R. (2015). Weather@homedevelopment and validation of a very large ensemble modeling system for probabilistic event attribution. *Quarterly Journal of the Royal Meteorological Society*, *141*(690), 1528–1545. <https://doi.org/10.1002/qj.2455>
- McCullagh, P., & Nelder, J. A. (1989). Generalized linear models. In *Monograph on Statistics and Applied Probability* (Vol. 37).
- Meinshausen, M., Smith, S. J., Calvin, K., Daniel, J. S., Kainuma, M. L. T., Lamarque, J.-F., ... van Vuuren, D. P. P. (2011). The RCP greenhouse gas concentrations and their extensions from 1765 to 2300. *Climate Change*, *109*(1–2, SI), 213–241. <https://doi.org/10.1007/s10584-011-0156-z>
- Mitchell, D., Heavyside, C., Vardoulakis, S., Huntingford, C., Masato, G., Guillod, B. P., Frumhoff, P., Bowery, A., Wallom, D., & Allen, M. (2016). Attributing human mortality during extreme heat waves to anthropogenic climate change. *Environmental Research Letters*, *11*(7). <https://doi.org/10.1088/1748-9326/11/7/074006>
- National Academies of Sciences, Engineering, and Medicine (2016). *Attribution of Extreme Weather Events in the Context of Climate Change*. National Academies Press.
- Orlowsky, B., & Seneviratne, S. I. (2013). Elusive drought: Uncertainty in observed trends and short- and long-term CMIP5 projections. *Hydrology and Earth System Sciences*, *17*(5), 1765–1781. <https://doi.org/10.5194/hess-17-1765-2013>
- Orth, R., Zscheischler, J., & Seneviratne, S. I. (2016). Record dry summer in 2015 challenges precipitation projections in Central Europe. *Scientific Reports*, *6*. <https://doi.org/10.1038/srep28334>
- Otto, F. E. L., Coelho, C. A. S., King, A., De Perez, E. C., Wada, Y., van Oldenborgh, G. J., ... Cullen, H. (2015). Factors other than climate change, main drivers of 2014/15 water shortage in Southeast Brazil. *Bulletin of the American Meteorological Society*, *96*(12), S35–S40. <https://doi.org/10.1175/BAMS-D-15-00120.1>
- Otto, F. E. L., Massey, N., van Oldenborgh, G. J., Jones, R. G., & Allen, M. R. (2012). Reconciling two approaches to attribution of the 2010 Russian heat wave. *Geophysical Research Letters*, *39*, L04,702. <https://doi.org/10.1029/2011GL050422>
- Polson, D., Bollasina, M., Hegerl, G. C., & Wilcox, L. J. (2014). Decreased monsoon precipitation in the northern hemisphere due to anthropogenic aerosols. *Geophysical Research Letters*, *41*(16), 6023–6029. <https://doi.org/10.1002/2014GL060811>
- Schaller, N., Kay, A. L., Lamb, R., Massey, N. R., van Oldenborgh, G. J., Otto, F. E. L., ... Allen, M. R. (2016). Human influence on climate in the 2014 southern England winter floods and their impacts. *Nature Climate Change*, *6*(6), 627–634. <https://doi.org/10.1038/NCLIMATE2927>
- Seneviratne, S. I., Nicholls, N., Easterling, D., Goodess, C., Kanae, S., Kossin, J., ... Zhang, X. (2012). *Changes in Climate Extremes and their Impacts on the Natural Physical Environment.*, book section 3. Cambridge, United Kingdom and New York, NY: Cambridge University Press.109230
- Shiogama, H., Watanabe, M., Imada, Y., Mori, M., Ishii, M., & Kimoto, M. (2013). An event attribution of the 2010 drought in the South Amazon region using the MIROC5 model. *Atmospheric Science Letters*, *14*(3), 170–175. <https://doi.org/10.1002/asl2.435>
- Sippel, S., Otto, F. E. L., Flach, M., & van Oldenborgh, G. J. (2016). The role of anthropogenic warming in 2015 central European heat waves. *Bulletin of the American Meteorological Society*, *97*, S51–S56. <https://doi.org/10.1175/BAMS-D-16-0150.1>
- Stagge, J. H., Tallaksen, L. M., Gudmundsson, L., Van Loon, A. F., & Stahl, K. (2015). Candidate distributions for climatological drought indices (SPI and SPEI). *International Journal of Climatology*, *35*(13), 4027–4040. <https://doi.org/10.1002/joc.4267>
- Stott, P., Stone, D., & Allen, M. (2004). Human contribution to the European heatwave of 2003. *Nature*, *432*(7017), 610614. <https://doi.org/10.1038/nature03089>
- Stott, P. A., Christidis, N., Otto, F. E. L., Sun, Y., Vanderlinden, J.-P., van Oldenborgh, G. J., ... Zwiers, F. W. (2016). Attribution of extreme weather and climate-related events. *Wiley Interdisciplinary Reviews-Climate Change*, *7*(1), 23–41. <https://doi.org/10.1002/wcc.380>

- Taylor, K. E., Stouffer, R. J., & Meehl, G. A. (2012). An overview of CMIP5 and the experiment design. *Bulletin of the American Meteorological Society*, 93(4), 485–498. <https://doi.org/10.1175/BAMS-D-11-00094.1>
- Thompson, A., & Otto, F. E. L. (2015). Ethical and normative implications of weather event attribution for policy discussions concerning loss and damage. *Climatic Change*, 133(3), 439–451. <https://doi.org/10.1007/s10584-015-1433-z>
- Uhe, P., Otto, F. E. L., Haustein, K., van Oldenborgh, G. J., King, A. D., Wallom, D. C. H., Allen, M. R., & Cullen, H. (2016). Comparison of methods: Attributing the 2014 record European temperatures to human influences. *Geophysical Research Letters*, 43(16), 8685–8693. <https://doi.org/10.1002/2016GL069568>
- van Haren, R., van Oldenborgh, G. J., Lenderink, G., Collins, M., & Hazeleger, W. (2013). SST and circulation trend biases cause an underestimation of European precipitation trends. *Climate Dynamics*, 40f(1–2), 1–20. <https://doi.org/10.1007/s00382-012-1401-5>
- Van Lanen, H. A. J., Laaha, G., Kingston, D. G., Gauster, T., Ionita, M., Vidal, J.-P., ... Van Loon, A. F. (2016). Hydrology needed to manage droughts: The 2015 European case. *Hydrological Processes*, 30(17), 3097–3104. <https://doi.org/10.1002/hyp.10838>
- van Oldenborgh, G. J. (2007). How unusual was autumn 2006 in Europe? *Climate of the Past*, 3(4), 659–668.
- Wilcox, L. J., Dong, B., Sutton, R. T., & Highwood, E. J. (2015). The 2014 hot, dry summer in northeast asia. *Bulletin of the American Meteorological Society*, 96(12), S105–S110. <https://doi.org/10.1175/bams-d-15-00123.1>
- Wilcox, L. J., Highwood, E. J., & Dunstone, N. J. (2013). The influence of anthropogenic aerosol on multi-decadal variations of historical global climate. *Environmental Research Letters*, 8(2). <https://doi.org/10.1088/1748-9326/8/2/024033>
- Xie, P., & Arkin, P. (1997). Global precipitation: A 17-year monthly analysis based on gauge observations, satellite estimates, and numerical model outputs. *Bulletin of the American Meteorological Society*, 78(11), 2539–2558. [https://doi.org/10.1175/1520-0477\(1997\)078<2539:GPAYMA>2.0.CO;2](https://doi.org/10.1175/1520-0477(1997)078<2539:GPAYMA>2.0.CO;2)